中國機械工程學刊第四十五卷第四期第 355~364 頁(民國一百一十三年)
Journal of the Chinese Society of Mechanical Engineers, Vol.45, No.4, pp355~364 (2024)

Numerical Analysis to Find Permeability of Lattice Structures

Pratik Prakash Gupta *, Sundararaj Senthilkumar **and Shung-Wen Kang ***

Keywords： Numerical analysis, Permeability, Porous structure, Octet.

ABSTRACT

As the need for efficient heat extraction grows with decreasing extraction areas, enhancing heat transfer device performance is crucial. Porous structures in thermal devices like heat pipes and vapor chambers can significantly improve heat transfer. Permeability, vital in fluid dynamics, affects fluid flow in porous materials, such as lattice structures. This study uses numerical analysis to assess the permeability of lattice structures, created using nTopology and analyzed with ANSYS Fluent software. It focuses on Octet, Isotruss, and Diamond lattice geometries. The research considers lattice geometry, unit cell characteristics, flow conditions, and other factors to deeply understand these structures' behavior. Insights into how different parameters influence lattice behavior and permeability are gained. The study also examines the impact of beam thickness and porosity on lattice performance. By varying and comparing these aspects, the study seeks to develop a more thorough framework for permeability research, contributing to advancements in lattice structure design and engineering applications.

INTRODUCTION

Porous structures are pivotal in various fields due to their unique properties, such as high surface area, tunable pore size, controlled porosity, and improved mass transport. These characteristics make

Paper Received September, 2023.Revised November,2023. Accepted November, 2023. Author for Correspondence:Shung-Wen Kang.

**Graduate Student, Department of Mechanical and Electro-Mechanical Engineering, Tamkang University, Tamsui, New Taipei City, Taiwan 251301.*

*** Professor, Department of Aerospace Engineering, SRM Institute of Science and Technology, Chennai, India.*

**** Professor, Department of Mechanical and Electro-Mechanical Engineering, Tamkang University, Tamsui, New Taipei City, Taiwan 251301.MechanicalEngineering, Tamkang University, Tamsui, New Taipei City,Taiwan 251301.*

This overview highlights the significance of previous wisdom, chemical engineering, biomedical engineering, energy storehouse, filtration, and catalysis. Previous accoutrements offer exceptional advantages similar as high face area, tunable severance size, controlled porosity, and enhanced mass transport, making them essential for a wide range of operations. The study by Bear and Braesterprevious wisdom, chemical engineering, biomedical engineering, energy storehouse, filtration, them integral in engineering, biomedical, energy storage, filtration, and catalysis. Highlighting the work of Bear and Braester (1972), the overview underscores the relevance of porous materials in contemporary engineering challenges and their potential for future developments. Numerical analysis has become a crucial tool in understanding and optimizing lattice structures, particularly in fluid dynamics, by allowing simulation of fluid flow and assessment of permeability impacts, thereby aiding design and engineering processes. Microporous materials like aerogels, known for their low thermal conductivity, are being investigated for their insulation potential. Komarneti (2007) studied points to new avenues for innovation, paving the way for improved functionality and performance in various applications.

The significance of pore structure in the mechanical properties of porous materials, combined with advances in technology allowing for complex pore structures, has spurred interest in their detailed characterization. This involves assessing parameters like porosity, pore distribution, types, aperture size, shape, tortuosity coefficients, pore size distribution, surface area, and permeability (Konovalenko et al., 2009; Smolin et al., 2014, 2019; Grigor'ev et al., 2017, 2018). Additive manufacturing, particularly in catalyst and sorbent material fabrication, offers enhanced design flexibility and the integration of multiple materials for improved functionality, potentially revolutionizing catalyst and sorbent fabrication for more efficient chemical processes (Rosseau et al. 2022).

The microstructure of porous scaffolds, similar to engineering foams, is crucial for their effectiveness, as detailed by Freyman et al. (2001), who also

discussed various fabrication methods and typical microstructures. Lattice structures, significant in fields like civil, aerospace, and biomechanics, are noted for their potential as ultra-stiff and strong metamaterials, with directionally controlled properties being vital for diverse applications (Xu et al., 2016; Meza et al., 2014). Egan et al. (2017) categorized unit cell structures in lattice designs into cubic, truncated, and octahedron families.

nTopology software, designed for additive manufacturing, offers solutions for lightweighting and strengthening designs, a long-standing engineering challenge. This software company specializes in advanced engineering design and simulation tools, using implicit modeling for creating complex, optimized geometries difficult with traditional CAD. Focused on additive manufacturing, nTopology enables efficient design, simulation, and optimization of intricate structures for lightweight, high-performance parts. This introduction underscores nTopology's role in advancing product design and manufacturing with innovative technologies.

Numerical analysis, particularly using ANSYS Fluent, a widely recognized finite modeling software, has been effectively employed to assess porous structures' properties. Key studies using ANSYS include evaluating permeability and tortuosity, showing good alignment with existing literature and highlighting the impact of fiber diameter and web thickness on tortuosity (Vallabh et al. 2011). Further, ANSYS Fluent has been used to analyze pressure drop in gas processing operations (Wahid et al. 2013) and to study heat transfer characteristics in porous structures, using the RANS model for 2D turbulent flow simulations (Hossain and Hossain, 2014). Xu et al. (2016) employed a multi-scale mathematical approach to analyze the permeability of metal fibers, revealing the significant influence of fractal topography on permeability.

Gauna and Zhao (2017) studied heat transfer in porous media for cooling, using ANSYS Fluent for simulating fluid flow in open-cell porous metals. They focused on varying porosity and its impact on permeability and heat transfer. Gangapatnam et al. (2018) analyzed forced convection in aluminum foams, contrasting LTE (Local Thermal Equilibrium) and LTNE (Local Thermal Non-Equilibrium) model conditions, validating their model against experiments. Dhinakar et al. (2021) examined the airflow in porous maraging steel made by selective laser melting, comparing ANSYS Fluent simulations with experimental data. Jafari et al. (2018) provided design guidelines for porous mold inserts in injection molding. These studies demonstrate the effectiveness of numerical simulation in assessing porous structures' flow and thermal properties.

This study focuses on three lattice structures: Octet, Isotruss, and Diamond. The Octet structure, typical in some ionic and covalent solids, features atoms surrounded by eight neighbors in a crystalline arrangement. Isotruss is a 3D lattice with interconnected struts forming triangular or tetrahedral elements in a repeating pattern. The Diamond structure, found in carbon's diamond allotrope, consists of carbon atoms in a face-centered cubic arrangement, with each atom covalently bonded to four others in a tetrahedral geometry. The study includes a detailed comparison of these unit cell structures.

The unit cell structures of Octet, Isotruss and Diamond cells are shown in Figure 1.

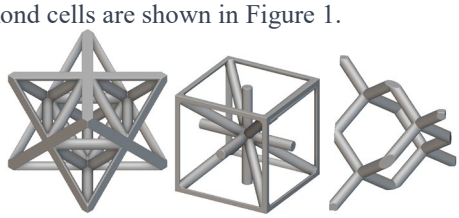

(A) (B) (C)

Fig. 1. The unit cell structure of a size of 10mm^3 and beam thickness of 2mm for (A) Octet. (B) Isotruss and (C) Diamond.

This paper emphasizes the importance of numerical simulation in evaluating and enhancing the properties of porous structures, particularly for industrial and research applications like vapor chambers, heat pipes, and heat exchangers. It focuses on using numerical analysis to determine the permeability of lattice structures, considering various factors such as lattice geometry, unit cell characteristics, and flow conditions to gain a comprehensive understanding of their behavior and permeability.

MATHEMATICAL MODELLING

In this study, the fluid flow and turbulence behavior is analyzed using the basic equations and continuity equations. The chosen model in Fluent is the k-ω turbulence model, which effectively handles the turbulence caused by flow through structures. Although the flow inlet is often in the laminar range, the k-ω model is used to account for any generated turbulence, which is expected to be moderate. This choice balances accuracy with model complexity, making it suitable for analyzing the intricate structures and flow dynamics involved.

The time averaged continuity equation is represented by equation 1,

$$\frac{\partial \bar{u}_i}{\partial x_i} = 0 \qquad (1)$$

The time averaged momentum equation is presented

in the equation 2,

$$\rho\bar{u}_j\frac{\partial\bar{u}_i}{\partial x_j} = \rho\bar{f}_i + \frac{\partial}{\partial x_j}[-\bar{p}\partial_{ij} + 2\mu\overline{S_{ij}} - \rho\overline{u_i'u_j'}] \quad (2)$$

In equation 2, the term Sij represents the strain tension in flow. The strain tension is given by formula in equation 3,

$$\overline{S_{ij}} = \frac{1}{2}\left(\frac{\partial\overline{u_i}}{\partial\overline{x_j}} + \frac{\partial\overline{u_j}}{\partial\overline{x_i}}\right) \quad (3)$$

The time averaged energy equation is given by equation 4,

$$U_i\frac{\partial\bar{T}}{\partial x_i} = \frac{\partial}{\partial x_i}\left(\alpha\frac{\partial\bar{T}}{\partial x_i} - \overline{u_i'T'}\right) + S \quad (4)$$

Where, ui, , uj is the directional velocity, xi , xj is the directional length, ρ is the density of fluid, T is the temperature, μ is the dynamic viscosity of fluid and S is the strain factor. In terms of direct analogy to the turbulent momentum equation for transport in energy, the turbulent heat transport is often assumed to be in direct correlation with the gradient of transport quantity. Equation 5 represents the gradient mentioned,

$$-\overline{u_i'T'} = \alpha_t\frac{\partial\bar{T}}{\partial x_i} \quad (5)$$

In equation 5 αt is the turbulent diffusivity of heat. Similar to eddy viscosity, αt is dependent upon the state of turbulence despite not being a property of fluid. By the Reynolds analogy between heat and mass we can conclude equation 6,

$$\alpha_t = \frac{v_t}{\sigma_t} \quad (6)$$

Here, the quantity σt is called the turbulent Prandtl or Schmidt number, where νt is the turbulent kinematic viscosity and σt is the turbulent surface tension. The standard k- ω model is based on the Wilcox model which incorporates modifications for low-Reynolds number effects, compressibility, and shear flow spreading One of the weak points of the Wilcox model is the sensitivity of the solutions to values for k and outside the shear layer (freestream sensitivity). The standard k- ω model is an empirical model based on model transport equations for the turbulence kinetic energy (k) and the specific dissipation rate (ω). As the k- ω model has been modified over the years, production terms have been added to both the k and ω equations, which have improved the accuracy of the model for predicting free shear flows.

The turbulence kinetic energy, k and the specific dissipation rate, ω are obtained from the following transport equations-

$$\frac{\partial}{\partial x_i}(\rho k u_i) = \frac{\partial}{\partial x_j}\left(\Gamma_k\frac{\partial k}{\partial x_j}\right) + G_k + Y_k + S_k \quad (7)$$

And

$$\frac{\partial}{\partial x_i}(\rho\omega u_i) = \frac{\partial}{\partial x_j}\left(\Gamma_\omega\frac{\partial\omega}{\partial x_j}\right) + G_\omega + Y_\omega + S_\omega \quad (8)$$

In these equations 7 and 8, Gk represents the generation of turbulence kinetic energy due to mean velocity gradients. Gω represents the generation of ω. Γk and Γω represent the effective diffusivity of k and ω respectively. Yk and Yω represent the dissipation of k and ω due to turbulence. Sk and Sω are user-defined source terms.

The effective diffusivities for the k- ω model are given by-

$$\Gamma_k = \mu + \frac{\mu_t}{\sigma_k} \quad 9)$$

$$\Gamma_\omega = \mu + \frac{\mu_t}{\sigma_\omega} \quad (10)$$

Where, σk and σω are the turbulent Prandlt numbers for k and ω.

For the modelling of turbulence production, we can look on both the production of k and ω separately. Production of k can be represented in terms of turbulence kinetic energy and can be defined by equation 11,

$$G_k = -\rho u_i u_j\frac{\delta u_j}{\delta x_i} \quad (11)$$

Where, Gk is the turbulence kinetic energy, u is a representation of velocity and x is the simultaneous direction in the 3-dimensional space.

We can define the term Gk in a similar term to Boussinesq hypothesis as equation 12. Boussinesq's hypothesis is that the turbulent stresses are related to the mean velocity gradients in almost the same way that the viscous stresses are related to the complete velocity gradients.

$$G_k = \mu_t S^2 \quad (12)$$

Where, S is the mean rate of strain tensor and can be defined as equation 13,

$$S = \sqrt{(S_i S_j)} \quad (13)$$

The production of ω can be defined as equation 14,

$$G_\omega = \alpha\frac{\omega}{k}G_k \quad (14)$$

Where, α is calculated by equation 15,

$$\alpha = \frac{\alpha_\infty}{\alpha^*}\left(\frac{\alpha_0 + \frac{Re_t}{Re_\omega}}{1 + \frac{Re_t}{Re_\omega}}\right) \quad (15)$$

Where, Re_ω= 2.295 x α*

Some of the constants in the given model can be taken for general uses are,

$\alpha_{\infty} = 1,$

$\alpha^{*} = 1.$

Boundary condition and discretization

For the boundary conditions of the numerical analysis the inlet is fixed with velocity inlet and outlet is taken as pressure outlet for all the designs. The other surfaces are taken as no slip wall condition with the actual geometry is also represented as no slip wall. The flow inlet of the surface is non developed flow which is changed from 1m/s to 10 m/s. The turbulence is turned on in the software and selected as the k-ω turbulence model. The flow characteristics of fluid, which is selected as water, were controlled by ANSYS Fluent software, and follow the given material properties in software. The governing equations are discretized using the finite volume method using Fluent. Pressure velocity coupling is achieved using the SIMPLEC algorithm. The pressure equation is discretized using a second-order scheme. The convective terms in the momentum equations are discretized using a second-order upwind scheme, and diffusion terms are discretized with a second-order scheme. A first-order implicit scheme is used for discretizing the temporal term. The y+ value for the wall function was maintained within the range of 5 to 10. The time step size (Δt) is chosen as 0.001 s. The flow is initialized with an operating pressure of 1 bar. The simulations are performed for a flow time of 100 s. the convergence criteria was taken as 10^{-5} for pressure output.

Assumptions

The numerical model is based on the comparative analysis design and thus the model itself was made to mimic the situations present in the experimental scenarios. The model in the simulation cannot replicate the exact conditions and variables present in the real world, so we need to have some variables in assumptions which can be divided into two sections. There will be assumptions for model used in the analysis as well as the assumptions which separates it to the experimental analysis while comparison. As explained in the last section the model used for this analysis is k-ω turbulence model, which has few assumptions we need to take in account. The assumption of the Fluent models is given here-

- Isotropic Turbulence: The model assumes that turbulence is isotropic, meaning that turbulence statistics are independent of direction. This assumption simplifies the modelling by assuming that the turbulence properties are only dependent on the local flow conditions.
- Reynolds-Averaged Navier-Stokes (RANS) Approach: The k-ω model belongs to the family of RANS models, which assumes that the turbulent flow variables can be separated into time-averaged and fluctuating components. It assumes that the statistical averages are sufficient to describe the flow behaviour.
- Boussinesq Hypothesis: The model employs the hypothesis, which assumes that the Reynolds stresses (turbulent stresses) are proportional to the mean velocity gradients and can be modelled using a turbulent viscosity.
- Local Equilibrium: The k-ω model assumes local equilibrium, meaning that the turbulence quantities reach a local balance between production, diffusion, and dissipation within each computational cell. This assumption allows for simplification and closure of the governing equations.

NUMERICAL ANALYSIS OF P0ROUS STRUCTURE

The objective of this analysis was to evaluate the permeability of lattice structures by employing different types of unit cell configurations. Additionally, an investigation was conducted to assess the impact of design constraints, such as the beam thickness of the unit cell and the flow length or lateral length of the lattice structure.

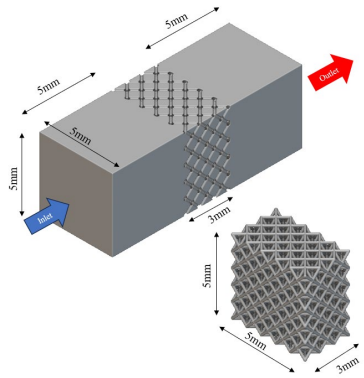

(A)

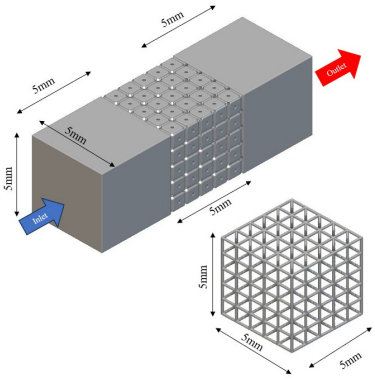

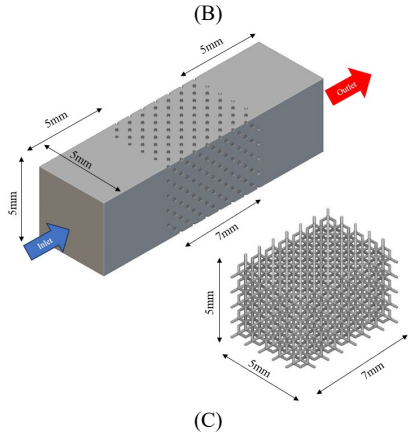

Fig. 2. The design of the domain and lattice of analysis is shown, where (A) Lattice length of 3mm of Octet structure (B) Lattice length of 5mm of Isotruss structure, and (C) Lattice length of 7mm of Diamond structure.

Figure 2 presents the design and dimensions of lattice structures within a specific analysis domain. It details the domain's length and the fixed 5mm lengths of both input and output sections. The flow is restricted to the lattice, with walls containing the fluid and directing it through the outflow boundary, ensuring no pressure loss or alteration in a stable state. Both the lattice and flow areas are consistently sized, creating a $5x5mm^2$ flow region within the lattice. Figure 2(A) shows an octet structure domain with a 3mm flow length and 0.15mm beam thickness. Figure 2(B) depicts a 5mm flow length with an Isotruss unit cell, while Figure 2(C) illustrates a 7mm flow length with a Diamond unit cell. These diagrams represent various unit cell types and lengths. Table 1 compiles all design variations.

Table 1. The diversity in designs and variables depends on the number of models.

Sample type	Sample unit cell size ($mm^{3)}$	Sample unit cell beam thickness (mm)	Beam thickness of sample in test (mm)	Inlet velocity (m/s)
Octet, Isotruss, Diamond	1x1x1	0.10 0.15 0.20	3, 5, 7	1 2 3 5 8 10

The study acknowledges several secondary variables that, while not primary, are critical for a thorough analysis of lattice structures. These factors significantly influence the characteristics and performance of the lattices. Including these variables in the analysis yields deeper insights into their effect on the lattice's overall behavior and permeability. This approach allows for an in-depth examination of how different elements, such as lattice geometry, unit cell properties, and flow conditions, interact and shape the system's behavior. Thus, considering these additional factors leads to a more complete and accurate evaluation of the lattice structure's performance and provides a nuanced understanding of its behavior under various conditions. Ultimately, this comprehensive approach enhances our understanding of the principles that govern the behavior of lattice structures.

The study focuses on the Octet, Diamond, and Isotruss lattice unit cell structures, with a particular emphasis on the impact of beam thickness on their mechanical properties and performance. Beam thickness, denoted as 'd' in Figure 3, refers to the cross-sectional thickness of the beams that make up the lattice structure. This dimension is a critical factor in determining the mechanical behavior of the lattice structures.

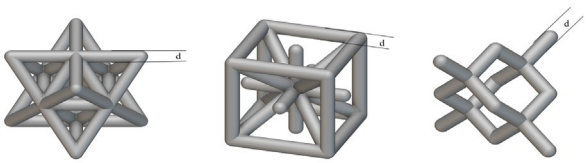

Fig. 3. Beam thickness (d) of a unit cell of a lattice structure (A) Octet,(B)Isotruss, and (C) Diamond.

The beam thickness in Octet and Diamond lattice structures is defined as the distance across the beam's faces or edges, typically measured perpendicular to the beam's direction. This dimension indicates the beams' width or breadth. In the Isotruss lattice, beam thickness refers to the cylindrical beams' diameter, representing their cross-sectional thickness. Beam thickness varies with design needs and manufacturing limits, significantly impacting the lattice's mechanical properties and performance. Thus, it's a key consideration in design and fabrication.

Another vital variable affecting analysis is lattice porosity, detailed in Table 2. Porosity, the voids within the lattice, influences permeability and fluid flow behavior. Adjusting porosity allows researchers to study its effect on permeability, enhancing understanding of flow dynamics changes with lattice porosity variations. This approach enables exploration of different permeability outcomes and determination of optimal porosity for improved fluid flow. Numerical analysis maintains consistent input parameters across all designs, as shown in Table 3.

Table 2. Porosity of the various design and unit cell structures for the numerical analysis.

Lattice structure	Beam thickness of unit cell (mm)	Porosity
Octet	0.10	0.9046
	0.15	0.7375
	0.20	0.5740
Isotruss	0.10	0.9465
	0.15	0.7907
	0.20	0.6521
Diamond	0.10	0.9496
	0.15	0.8915
	0.20	0.7624

Table 3. Input parameters for the numerical analysis model in ANSYS Fluent.

Fluent input	Lattice length	Mesh Count
Mesh size	3mm	~550,000
	5mm	~750,000
	7mm	~920,000
	Value	
velocity	1 m/s, 2m/s, 3m/s, 5m/, 8m/s and 10m/s	
fluid and density	Water – 998.2kg/m^3	
Flow model	*k*- ω SST viscus flow	
Flow time	100 seconds	

RESULTS AND DISCUSSIONS

The model assesses the permeability of lattice structures with varying flow inlets, a key property in fluid dynamics typically evaluated through forced flow tests using liquids or gases. In these tests, a known pressure drop is applied, and the resultant flow rate is measured. For liquid flow in wicks, like water at low velocities, Darcy's law becomes applicable due to negligible inertial forces, enabling accurate permeability measurement. This law establishes a linear relationship between flow rate and pressure drop in porous media, allowing determination of the permeability constant. In heat transfer applications, wick permeability is crucial for liquid transport efficiency. By conducting forced flow tests - applying a specific pressure drop and measuring the flow rate - the permeability of wick materials can be precisely determined. This knowledge is essential in designing and optimizing thermal devices, as permeability impacts liquid transport efficiency and overall system performance.

The Darcy law is given by equation 16,

$$\frac{\Delta P}{L} = \frac{\mu}{K} v \tag{16}$$

The formula involves ΔP (pressure drop), L (lateral flow length), v (effective velocity), μ (dynamic viscosity of the fluid), and K (effective permeability of the porous structure). Using this equation, permeability is calculated by first determining the pressure drop across the flow volume, then applying equation 16 with various input variables.

Validation of model

Mesh dependency validation in ANSYS Fluent fluid flow models is essential for ensuring simulation accuracy and reliability. This process, which discretizes the computational domain into elements to capture flow behavior, involves assessing the impact of different mesh resolutions on simulation results. It ensures convergence, stability, and reliability by determining the necessary refinement level to minimize mesh resolution dependency. This balance is crucial for achieving accurate solutions while maintaining computational efficiency. Validation also includes comparing simulation outcomes with experimental or analytical data to evaluate model robustness and identify potential issues with specific mesh resolutions.

For mesh independence validation, a consistent octet mesh design with a 3mm lateral length and a 0.15mm beam thickness was tested across four mesh sizes under the same input conditions and an inlet velocity of 1m/s. The tests measured pressure drop and calculated permeability using the same equation, revealing the impact of grid size or chosen mesh on permeability. The results of the mesh validation test, including visual contours, are presented in Table 4 and Figure 4.

Table 4**.** The result of the validation study.

Structure	Size (mm^3)	Mesh number	Output permeability (m^2)	Run time (hours)
octet	5×5×3	245365	9.50×10^{-09}	4.0
	5×5×3	568421	9.57×10^{-09}	6.5
	5×5×3	865412	9.57×10^{-09}	10.0
	5×5×3	1236514	9.57×10^{-09}	16.0

The results indicate minimal variation in both velocities and pressure drop profiles across different mesh sizes. Although these differences are visually indiscernible, permeability calculations reveal slight changes when transitioning from very coarse to medium mesh sizes. The differences between medium, fine, and very fine meshes are negligible. Notably, runtime increases with finer mesh resolutions. Therefore, using a medium mesh size is recommended for efficient simulation, providing satisfactory results without compromising output quality. Additionally, running models in parallel can save time by processing multiple simulations simultaneously.

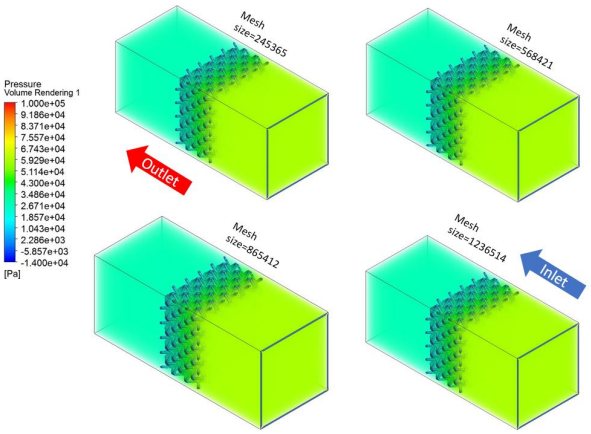

(A)

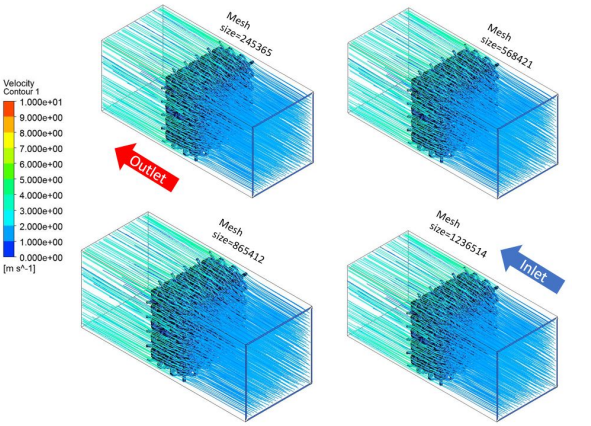

(B)

Fig. 4. (A) The pressure profile of mesh structures with varying sizes, and (B) The velocity profile of the differently sized mesh structures.

Permeability results

For permeability results, numerical analyses were conducted for various structure types, beam thicknesses, and lateral flow lengths as outlined in Table 1. The results, allowing for comparison and understanding of the significance of each variable change, are presented as follows: For the Octet structure, permeability results with beam thicknesses of 0.1mm, 0.15mm, and 0.2mm are shown in Figures 5(A), 5(B), and 5(C) respectively. For the Isotruss structure, results for beam thicknesses of 0.1mm, 0.15mm, and 0.2mm are depicted in Figures 6(A), 6(B), and 6(C) respectively. For the Diamond structure, the results for beam thicknesses of 0.1mm, 0.15mm, and 0.2mm are illustrated in Figures 7(A), 7(B), and 7(C) respectively.

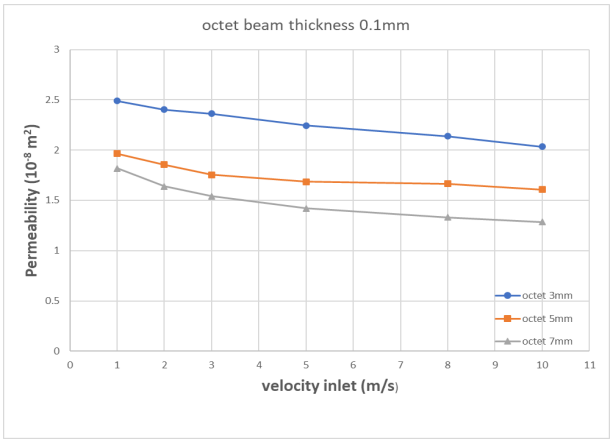

(A)

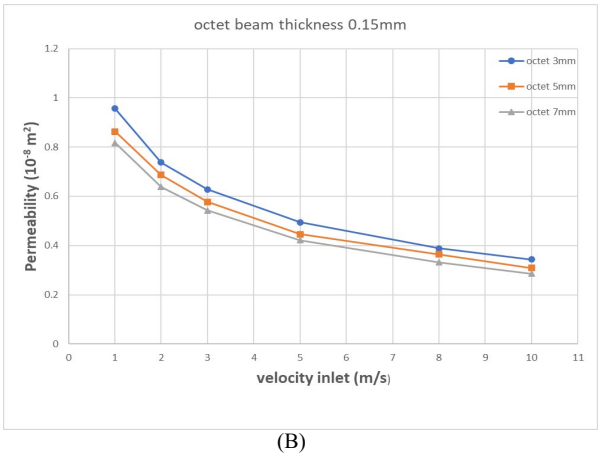

(B)

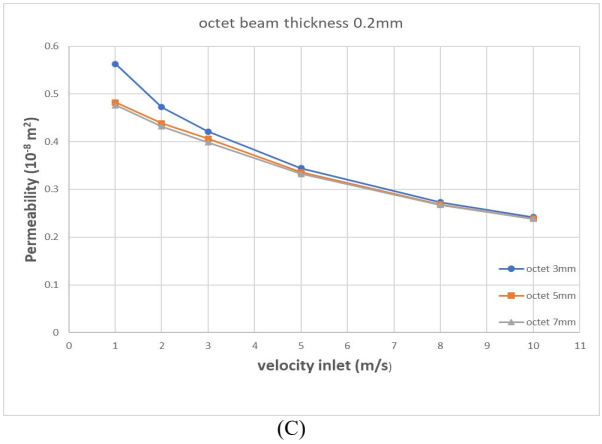

(C)

Fig. 5. The permeability of Octet structure with different lateral flow length of 3mm, 5mm and 7mm and with beam thickness (A) 0.1mm, (B) 0.15mm and (C) 0.2mm.

The study also compares permeabilities of the same lattice structure at different input velocities and various lateral flow lengths. The results of these comparisons are presented in Figure 8, with subfigures 8(A) to 8(E) corresponding to inlet velocities of 1m/s, 3m/s, 5m/s, 8m/s, and 10m/s, respectively.

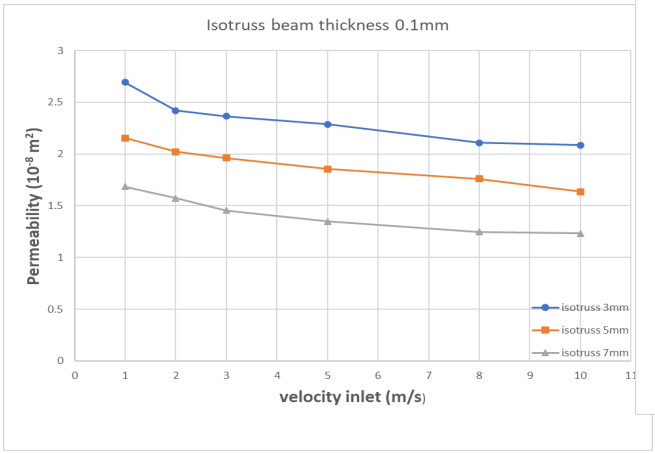

(A)

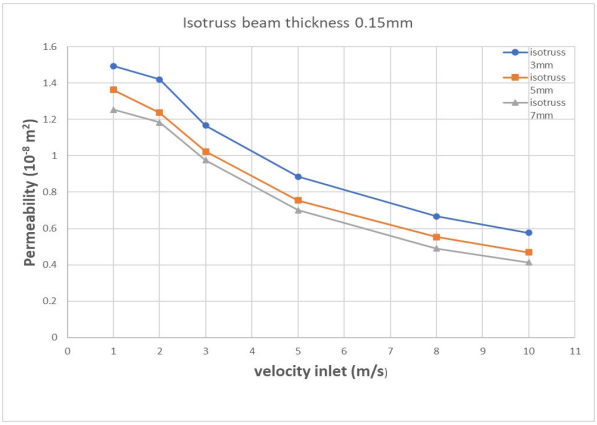

(B)

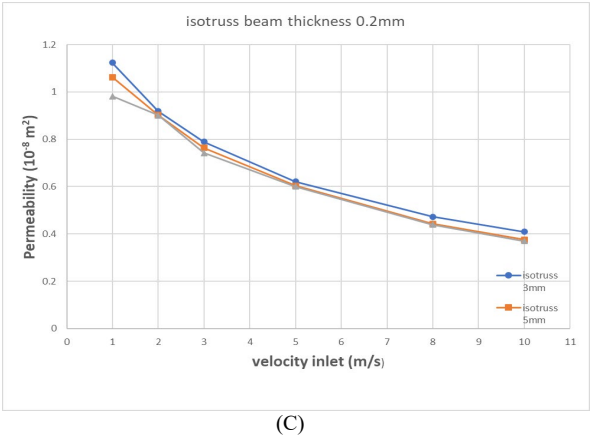

(C)

Fig. 6. The permeability of Isotruss structure with different lateral flow length of 3mm, 5mm and 7mm and with beam thickness (A) 0.1mm, (B) 0.15mm and (C)0.2mm.

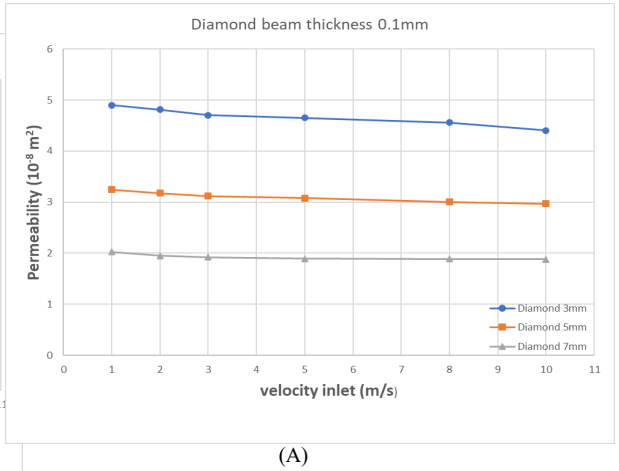

(A)

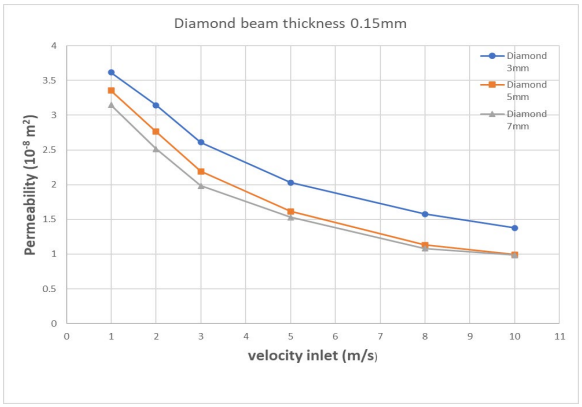

(B)

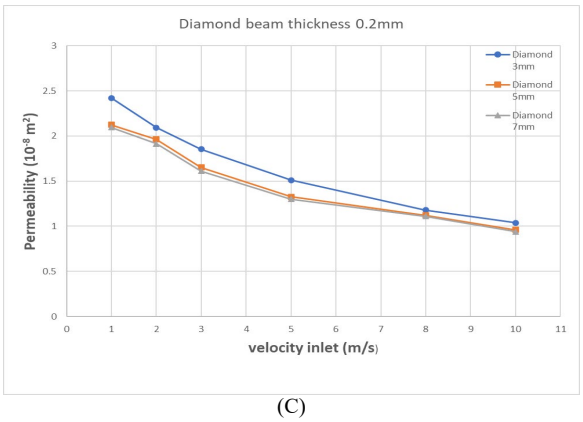

(C)

Fig. 7. The permeability of Diamond structure with different lateral flow length of 3mm, 5mm and 7mm and with beam thickness (A) 0.1mm, (B) 0.15mm and (C) 0.2mm.

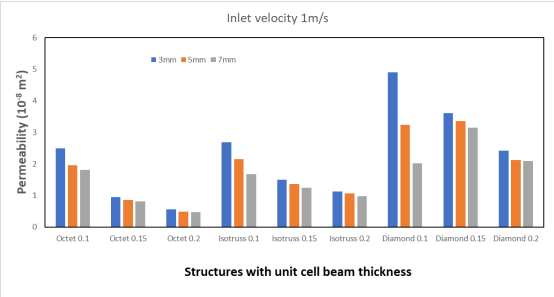

(A)

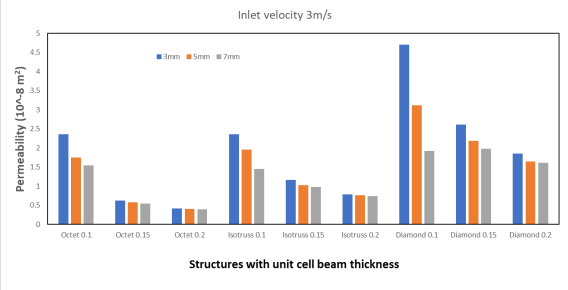

(B)

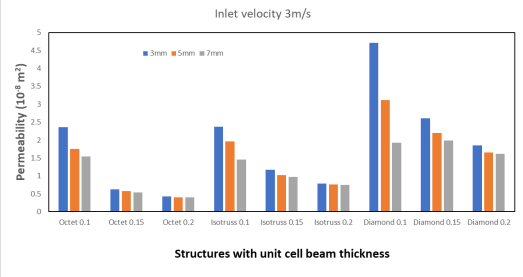

(C)

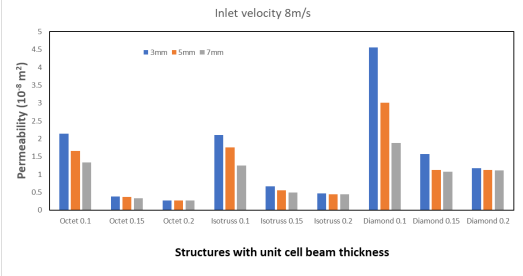

(D)

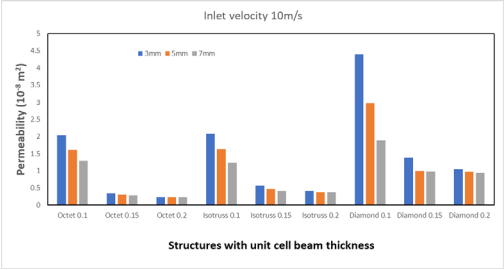

(E)

Fig. 8. Permeability of structures at different inlet velocity of (A) 1m/s, (B) 3m/s, (C) 5m/s, (D) 8m/s, and (E) 10m/s.

The study observes how changing input conditions impact pressure and velocity in lattice structures, focusing on a single velocity for consistency. It finds that permeability decreases with higher inlet velocities and longer lateral flows, showing an inverse relationship with these factors. However, the impact of lateral flow length is less significant than velocity. Beam thickness is also crucial; as it increases, porosity and therefore permeability decrease. The study highlights the need for a balance between manufacturability, porosity, and structural integrity for optimal permeability in lattice structures

CONCLUSIONS

Permeability is significantly influenced by factors like beam thickness, lateral flow length, and velocity in lattice structures. An increase in beam thickness reduces porosity and permeability. This impact is more pronounced in low-porosity structures such as Octet compared to high-porosity ones such as Diamond. Extended lateral flow lengths lower permeability due to increased pressure drop and diminished flow efficiency, especially when combined with increased beam thickness. Among lattice structures, Diamond has the highest permeability, followed by Isotruss, with Octet being the least permeable. Permeability is inversely related to fluid flow velocity; higher velocities indicate reduced flow efficiency and increased resistance within the lattice. This numerical analysis aids in understanding permeability trends and in selecting parameters for optimizing lattice structures.

ACKNOWLEDGMENT

Financial support for this work was provided by the Ministry of Science and Technology of Taiwan, ROC under the contract NSTC 112-2221-E-032-026

REFERENCES

Bear, J., and Braester, C. “On the flow of two immiscible fluids in fractured porous media,” Developments in Soil Science, Vol. 2, pp. 177-202 (1972).

Dhinakar, A., Li, B. E., Chang, Y. C., Chiu, K. C. and Chen, J. K., “Air permeability of maraging steel cellular parts made by selective laser melting,”; Materials, Vol. 14, no. 14113118 (2021).

Egan, P. F., Gonella, V. C., Engensperger, M., Ferguson, S. J. and Shea, K., J PloS one. “Computationally designed lattices with tuned properties for tissue engineering using 3D printing,”, PLOS ONE, no. 0182902 (2017).

Freyman, T.M., Yannas, I. V. and Gibson, L. J., “Cellular Materials as Porous Scaffolds for Tissue Engineering,”; Progress in Materials Science, Vol.46, pp. 273-282 (2001).

Gangapatnam, P., Kurian, R. and Venkateshan, S. P., . “Numerical simulation of heat transfer in metal foams,”; Heat and Mass Transfer, Vol. 54, pp. 553-562 (2018).

Gauna, E. A. and Zhao, Y.,. “Numerical simulation of heat transfer in porous metals for cooling applications,”; Metallurgical and Materials Transactions B, Vol. 48, pp. 1925-1932 (2017).

Grigor’ev, M. V., Savchenko, N. L., Buyakova, S. P. and Kul’kov, S. N., “Inelastic behavior of ceramics with hierarchical pore structure under compression,”; Technical Physics Letters, Vol. 43, pp. 723-726 (2017).

Grigor’ev, M. V., Savchenko, N. L., Sablina, T. Y., Kurovics, E., Sevostyanova, I. N., Buyakova, S. P., Gömze, L. A. and Kulkov, S. N.,. “Deformation and fracture of alumina ceramics with hierarchical porosity,”; Journal of Silicate Based and Composite Materials, Vol. 70, pp. 18-22 (2018).

Hossain, M. A. and Hossain, A., “Numerical investigation of porous medium heat transfer,”; Proceedings of ASME International Mechanical Engineering Congress and Exposition. (2014).

Jafari, D., Wits, W. W. and Geurts, B. J., “Metal 3D-printed wick structures for heat pipe application: capillary performance analysis,”; Applied Thermal Engineering, Vol. 143, pp. 403-414 (2018).

Komarneni, S. “Porous materials: science and engineering,”; Materials Research Innovations., Vol. 11, pp. 37-38 (2007).

Konovalenko, I. S., Smolin, A. Y., Korostelev, S. Y., and Psakh’e, S. G. “Dependence of the macroscopic elastic properties of porous media on the parameters of a stochastic spatial pore distribution,”; Technical Physics, Vol. 54, pp. 758-761 (2009).

Meza, L., R, Satyajit Das, S. and Greet, J. R., “Strong, lightweight, and recoverable three-dimensional ceramic nanolattices,”; Science, 2014, Vol: 345, pp. 1322-1326 (2014).

Rosseau, L. R. S., Middelkoop, V., Willemsen, H. A. M., Roghair, I. and Annaland, M. V., S.,“Review on additive manufacturing of catalysts and sorbents and the potential for process intensification,”.; Frontiers in Chemical Engineering, Vol: 4, no. 834547: 3389 (2022).

Smolin, A. Y., Roman,N. V.,Konovalenko, I. S., Eremina, G. M.,Buyakova, S. P. and Psakhie, S. G. “3D simulation of dependence of mechanical properties of porous ceramics on porosity,“; Engineering Fracture Mechanics. 2014, Vol. 130, pp. 53-64 (2014).

Smolin, A. Y., GM Eremina, G. M. and Korostelev, S. Y. “Methods for describing structure of novel porous materials: A review,” Proceedings of IOP Conference Series: Materials Science and Engineering (2019).

Vallabh, R., Ducoste,J., Seyam, A. F. and Pamela B. L., “Modeling tortuosity in thin fibrous porous media using computational fluid dynamics,”; Journal of Porous Media, Vol. 14, pp. 791-804 (2011).

Wahid, S., Cahela, D. R. and Tatarchuk, B. J., “Experimental, theoretical, and computational comparison of pressure drops occurring in pleated catalyst structure,”; Industrial and Engineering Chemistry Research, Vol. 52, pp. 14472-14482 (2013).

Xu, S., Shen, J., Zhou, S., Huang, X. and Xie, Y. M., “Design of lattice structures with controlled anisotropy,”; Materials and Design, Vol. 93, pp. 443-447 (2016).

Xu, Z. J., Wang, Q. H., Yang, S. and Li, J. R., “Active multi-scale modeling and gas permeability study of porous metal fiber sintered felt for proton exchange membrane fuel cells,”; International Journal of Hydrogen Energy, Vol. 41, pp. 7393-7407 (2016).

晶格結構滲透性數值分析

古佩笛 康尚文
淡江大學機與機電工程學系

Sundararaj Senthilkumar
印度蘭馬斯瓦米紀念大學航空太空工程學系

摘 要

面對日益增長的排熱需求和空間限制，提升熱傳設備效率迫切。本研究利用多孔材料結構改進熱管和蒸汽腔體性能，特別關注流體滲透性對晶格結構的影響。使用 ANSYS Fluent 軟體進行滲透性模擬，包括八面體、Isotruss 和鑽石型晶格。考慮晶格幾何、單元格特性、流體條件等因素，深入探討各參數對滲透性的影響，同時研究樑厚度和孔隙率對晶格性能的影響。透過系統性分析，旨在建立全面的架構，研究和調控滲透性，推動晶格結構在工程應用中的發展。